

## Identification of Death-Associated Protein Kinases Inhibitors Using Structure-Based Virtual Screening<sup>†</sup>

Masako Okamoto,<sup>\*,‡</sup> Kiyoshi Takayama,<sup>§</sup> Tomoko Shimizu,<sup>§</sup> Kazuhiro Ishida,<sup>‡</sup> Osamu Takahashi,<sup>‡</sup> and Toshio Furuya<sup>‡</sup>

<sup>‡</sup>*Drug Discovery Department, Research and Development Division, PharmaDesign, Inc., 2-19-8 Hatchobori, Chuo-ku, Tokyo 104-0032, Japan, and* <sup>§</sup>*NB Health Laboratory Co. Ltd., A1-551 12-18, Kamiaoki 3, Kawaguchi City, Saitama 333-0844, Japan*

Received August 11, 2009

Death-associated protein kinases (DAPKs) function in the early stages of eukaryotic programmed cell death. DAPKs are now emerging as targets for drug discovery in novel therapeutic approaches for ischemic diseases in the brain, heart, kidney, and other organs. Using a structure-based virtual screening approach, we discovered potent and selective DAPKs inhibitors. **6** was found to be the most potent inhibitor with enzyme selectivity ( $IC_{50} = 69$  nM for DAPK1).

### Introduction

There has been significant scientific progress in the interpretation of so-called programmed cell death. During the past decade, various signaling molecules have been reported to be involved in this process. Among such studies, Kimchi et al. at the Weizmann Institute of Science in Israel identified a new serine/threonine kinase and designated it as death-associated protein kinase (DAPK<sup>a</sup>) because of its significant involvement in programmed cell death.<sup>1</sup> Subsequently, other serine–threonine kinases with significant homology in their kinase regions were identified and also designated DAPKs. At present, the DAPK family consists of at least five protein kinases: DAPK1, DAPK2, DAPK3, DRAK1, and DRAK2.<sup>2</sup>

These kinases play a central role in programmed cell death such as apoptosis and autophagy. The initially identified kinase in the family, DAPK (now known as DAPK1), is an ideal protein for understanding the significance of potential targets for novel drug development. It has been reported that DAPK1 is activated in nerve cells of the ischemic rat brain. In addition, DAPK1-defective neurocytes in the rat hippocampus show resistance to ceramide-induced cell death. These results strongly suggest that inhibition of DAPK1 and its related kinase activation has therapeutic relevance in the treatment of brain infarction and acute coronary ischemic diseases.<sup>3,4</sup> In fact, Velentza et al. at Northwestern University in Chicago reported that a nonselective inhibitory compound for DAPK1 significantly reduced ischemic damage in a rat brain ischemic model after a single injection, even at 6 h after the ischemic event.<sup>5</sup> However, potent and enzyme-selective DAPK inhibitors have not yet been identified.

In the past several years, we have used customized in-house programs based on structure-based virtual screening (SBVS). These include CONSENSUS-DOCK, a customized version

of the DOCK4 program,<sup>6</sup> in which three scoring functions (DOCK4, FlexX,<sup>7</sup> and PMF<sup>8</sup>) and consensus scoring<sup>9</sup> have been implemented. With this method, we were successful in identifying potent agonists/antagonists or inhibitors for several target proteins (e.g., GPCR, kinase, etc.) from a database containing millions of commercially available compounds.<sup>10</sup> In this paper, we report the application of CONSENSUS-DOCK for finding novel DAPKs inhibitors using an SBVS approach.

In this approach, preparation of an appropriate three-dimensional protein structure is essential to obtain accurate results in virtual screening. In the case of kinases, many kinases have several X-ray crystal structures that can be used for SBVS easily. However, we generated protein–ligands complex models by molecular dynamics (MD) simulation to identify compounds that have novel scaffolds and to increase the efficiency of screening large-scale databases of compounds.

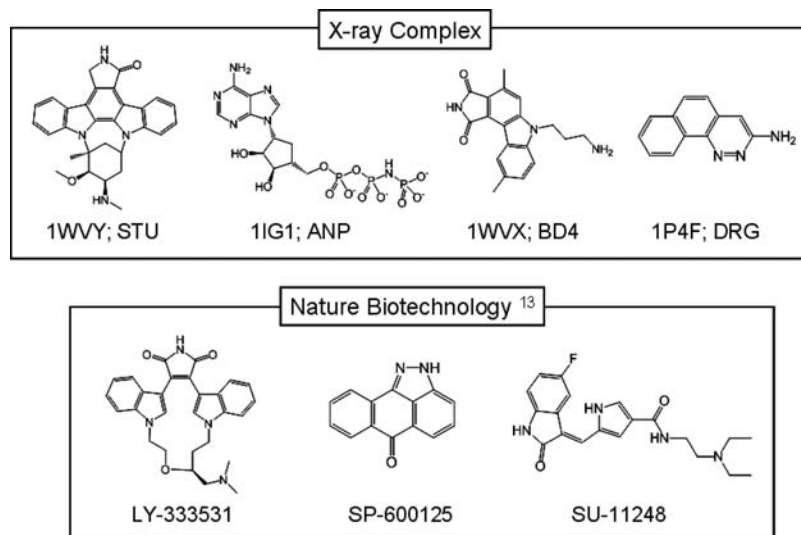
### Results and Discussion

**Preparation of the Binding Site Model.** Although there were several X-ray crystal complex structures of DAPK (1IG1,<sup>11</sup> 1JKK,<sup>11</sup> 1JKL,<sup>11</sup> 1P4F,<sup>5</sup> 1WVX, and 1WVY) at the beginning of our research, we constructed a protein–ligands complex model with an X-ray crystal structure (PDB code 1WVX) and four ligands observed in crystal complex structures (ANP, 1IG1; DRG, 1P4F; BD4, 1WVX; and STU, 1WVY; Figure 1) using MD simulation to gain better enrichment in virtual screening. In this study, we used a molecular dynamics simulation module in MOE<sup>12</sup> (Chemical Computing Group Inc., Montreal, Canada) by modifying an SVL script to build the complex models. This SVL script, called MultiCopyMD, was devised to enable several ligand molecules to be positioned in the binding site of the target protein simultaneously during the simulation so that the consensus binding conformation of that protein for multiple ligands can be generated. Intermolecular forces between the protein and each ligand are divided by the number of ligands included in the calculation, and intermolecular forces among the ligands are excluded in the MultiCopyMD simulation. Water molecules were soaked

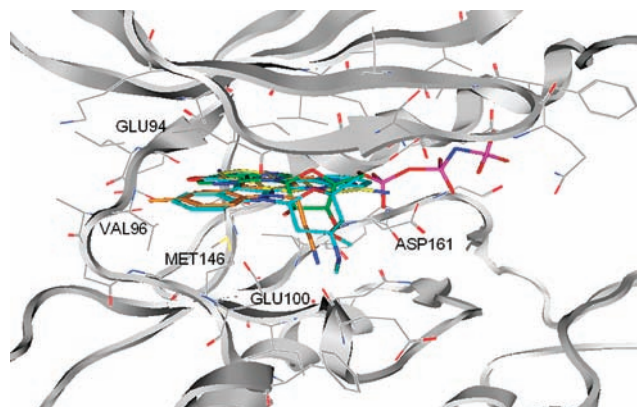
<sup>†</sup>PDB codes for ligands used in protein–ligand model: 1IG1, 1P4F, 1WVX, 1WVY.

\*To whom correspondence should be addressed. Phone: +81-3-3523-9630. Fax: +81-3-3523-9631. E-mail: okamoto@pharmadesign.co.jp.

<sup>a</sup>Abbreviations: DAPK, death-associated protein kinase; SBVS, structure-based virtual screening; MOE, molecular operating environment.



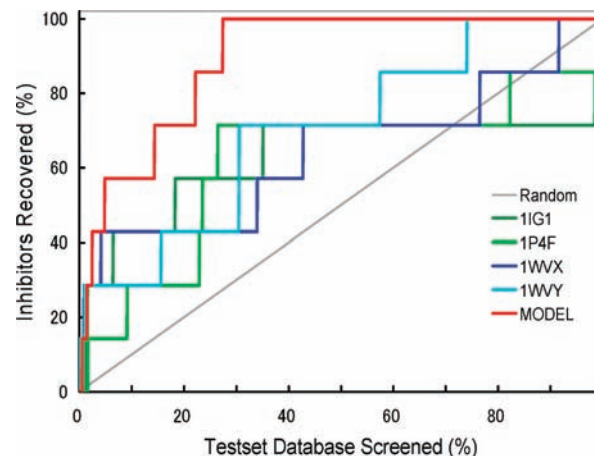
**Figure 1.** DAPK ligands and inhibitors. Four compounds (ANP, DRG, BD4, and STU) in X-ray crystal complex structures were used to make a complex model. These four compounds and three additional compounds (LY-333531, SP-600125, and SU-11248) with reported DAPK inhibition activity<sup>13</sup> were used in the small-scale (approximately a 1000-compound test set database) virtual screening using CONSENSUS-DOCK.



**Figure 2.** Structure of the DAPK–ligands complex model built by MultiCopyMD. Ligands are ANP (light-green, PDB code 1IG1), DRG (yellow, PDB code 1P4F), BD4 (orange, PDB code 1WVX), and STU (light-blue, PDB code 1WVY).

within 20 Å of the center of the ligands in the complex model with wall restraints around them, while the side chain atoms within 4.5 Å of the center of the ligands and the backbone atoms of the glycine-rich loop were unfixed in the MD calculations. The system was gradually heated to 300 K, and an additional 1 ns simulation at constant temperature and volume (NVT ensemble, NPA algorithm) was carried out. We then clustered the coordinates in this trajectory and selected several structures to compare each enrichment of virtual screening. One of the complex model structures is shown in Figure 2.

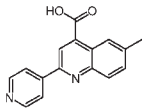
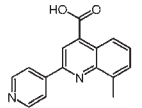
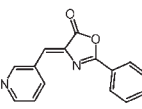
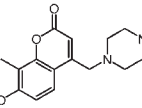
**Virtual Screening Using CONSENSUS-DOCK.** We compared the enrichments among protein structures (X-ray crystal complex structures and complex model structures built by MD simulation) by small-scale (approximately a 1000-compound test set database) virtual screening using CONSENSUS-DOCK. These 1000 compounds were selected randomly from the commercially available compound databases, filtered by druglikeness and clustering. The small-scale testset database has these 1000 compounds and 4 ligands of the X-ray crystal complex structures (1IG1, DRG; 1P4F, BD4; 1WVX, STU; and 1WVY), as well as



**Figure 3.** Comparison of enrichment curves for protein structures (complex model built by molecular dynamics simulation, using X-ray crystal complex structures 1IG1, 1P4F, 1WVX, 1WVY). The “MODEL” structure has the best enrichment among other model structures selected in the trajectory of molecular dynamics simulation.

three kinase inhibitors (SP600125, SU11248, and LY333531) reported by Fabian et al.<sup>13</sup> (Figure 1) to have DAPK inhibition activity. We found that a complex model structure had the best enrichment (Figure 3) among the X-ray crystal complex structures and other model structures. Thus, we decided to adopt this structural model built by MD simulation for large-scale (approximately a 400 000-compound database) virtual screening. For more efficient virtual screening, we typically use several hundreds of thousands compounds that have been refined using druglikeness filtering (reported by Hirayama et al.<sup>14</sup>) and clustered using principle components analysis (PCA) on the basis of the MACCS feature counts by MOE, from over millions of commercially available compounds.<sup>10</sup> For each compound in the database, after molecules were washed (salt disconnection, removal of minor components, deprotonation of strong acids, and protonation of strong bases) by MOE, the three-dimensional structure generator CORINA<sup>15</sup> (version 3.10) was used to

**Table 1.** Structures of Four Compounds Exhibiting Greater than 50% Inhibition at 10  $\mu$ M in the First Virtual Screening

Compound		DAPK3 %Inhibition at 10 $\mu$ M	DAPK3 %Inhibition at 1 $\mu$ M
1		58%	3%
2		72%	2%
3		84%	71%
4		54%	12%

calculate three-dimensional structures, including stereoisomers.

In CONSENSUS-DOCK, three scoring functions (DOCK4, FlexX, and PMF) may be implemented in the DOCK4 program and consensus scoring is performed in the pose selection and the ranking of compounds to complement the weaknesses of each scoring function. CONSENSUS-DOCK calculates these three scoring functions simultaneously. The consensus score of score 1, score 2, and score 3 is defined by  $\text{MAX}(\text{score 1, score 2, score 3})$ , where  $\text{MAX}()$  means the maximum value among the arguments. In other words, we chose the most unfavorable value from the three scores. By use of this definition of consensus score, each scoring functions complements the others by hiding artificial minimums of each scoring functions and false positives are decreased in the screening. This methodology can bring better results in virtual screening than using DOCK4 alone (see Supporting Information). After the calculations of CONSENSUS-DOCK were generated, we selected 602 compounds by consensus scoring<sup>9</sup> (docking score of CONSENSUS-DOCK), binding mode, and visual inspection. Furthermore, for the kinase inhibition assay, we selected 100 of the initial 602 compounds by optimizing the protein–ligands complex structures using quantum mechanics/molecular mechanics methods<sup>16</sup> to allow three scientists to visually inspect the compounds and select those compounds having a suitable binding mode at the ATP binding site. The outputs of CONSENSUS-DOCK are not done enough optimization because the calculation time for each compound was reduced to calculate the large number of compounds (around 400 000) in the database. The optimization steps were thought to improve the results.

**In Vitro Assay of Kinase Inhibitory Activity after First Virtual Screening.** The compounds selected by virtual screening were tested in a DAPK3 inhibition assay, and seven compounds showed appreciable inhibition at 10  $\mu$ M. Four of these seven compounds exhibited greater than 50% inhibition at this concentration (Table 1). Even at a final concentration of 1  $\mu$ M, **3** and **4** reduced DAPK3 enzyme activity by 71% and 12%, respectively.

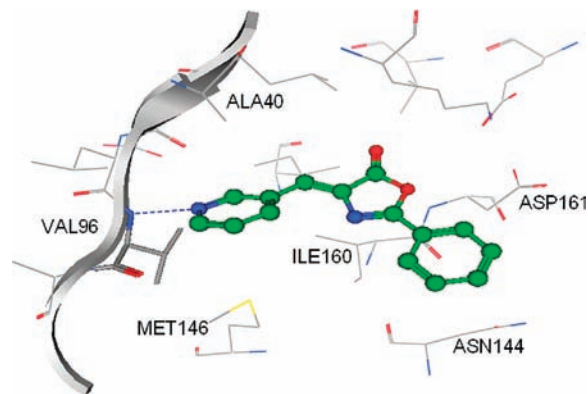


**Figure 4.** Computational docking of **3** to the active site of the DAPK catalytic subunit. This predictive binding mode was calculated by CONSENSUS-DOCK. Compound **3** forms a hydrogen bond between the nitrogen in the pyridinyl group and the backbone NH of Val96 in the hinge region. Furthermore, hydrophobic interactions (involving Ala40, Met146, and Ile160) likely play a role in the binding between **3** and DAPK.

The predicted binding mode of **3** in the active site of the DAPK catalytic domain is shown in Figure 4. In this binding mode, **3** forms a hydrogen bond between the nitrogen in the pyridinyl group and the backbone NH of Val96 in the hinge region. Furthermore, some hydrophobic interactions (involving Ala40, Met146, and Ile160) can be considered between **3** and DAPK. These hydrogen bonds and hydrophobic interactions should contribute to the stabilization of the complex between **3** and the DAPK kinase domain.

**Second Screening (Similarity Search).** To increase the inhibitory activity of the most potent hit compound (**3**) in the first virtual screening, we carried out a similarity search against the millions of commercially available compounds in the database. We first calculated a fingerprint based on the descriptors of the BIT\_MACCS:MACCS structural keys for the database and then carried out a similarity search using **3** as a query. Through these steps and visual inspection, we selected 39 compounds, which were subsequently purchased from several suppliers.

These 39 compounds were tested in the second DAPK inhibition assay, and 20 of these showed appreciable inhibition at 10  $\mu$ M. At this concentration, 16 compounds exhibited greater than 50% inhibition. Four representative compounds are shown in Table 2. Several compounds selected in the second screening showed more potent inhibitory activity than **3**, probably because of the additional hydrophobic interactions in the ATP binding cavity as a result of substituting the bulkier phenyl group in **3**. These compounds were subjected to subtype DAPK inhibition assay and showed potent inhibitory activity against DAPK1 and DAPK3 (Table 2). We found that **6** was the most potent DAPK inhibitor among those tested compounds in this study. The inhibitory profile of **6** was then examined. When assayed with 10  $\mu$ M ATP, the  $\text{IC}_{50}$  values for DAPK1 and DAPK3 were 69 and 225 nM, respectively (parts A and C of Figure 5). The inhibition kinetics of **6** confirmed that the compound is a competitive inhibitor of ATP substrate against DAPK1 and DAPK3 (parts B and D of Figure 5B). To test the enzyme selectivity of **6**, a kinase panel assay was carried out using ProfilerPro Kits (Caliper Life Sciences, Inc., Hopkinton, MA). As shown in Table 3, **6** appeared to be a specific inhibitor of DAPK with respect to

**Table 2.** Structures of Four Representative Compounds in Second Screening<sup>a</sup>

Compound	Structure	DAPK1 %Inhibition at 10 $\mu$ M	DAPK3 %Inhibition at 10 $\mu$ M
5		89%	45%
6		91%	100%
7		90%	100%
8		98%	96%

<sup>a</sup>These compounds show potent inhibition of DAPK1 and DAPK3.

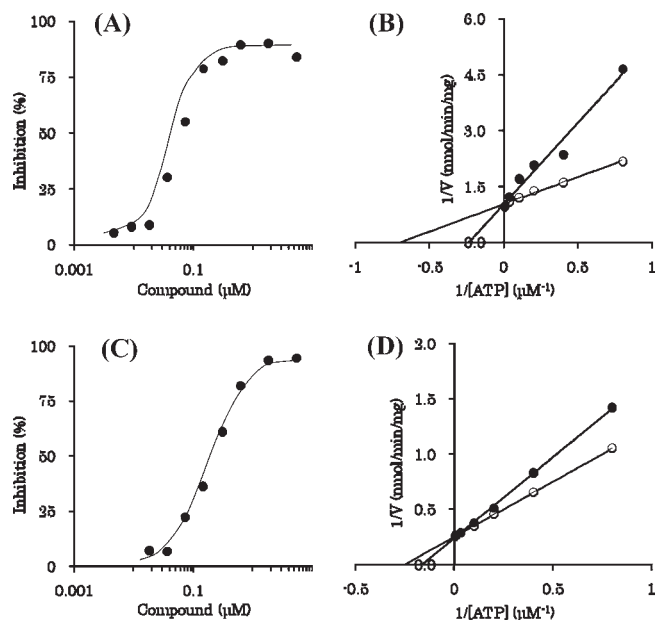


**Figure 5.** Inhibition kinetic analysis of **6**. DAPK1 (A) and DAPK3 (C) were incubated in the presence of 10  $\mu$ M ATP and various concentrations of **6**. Enzyme activities of DAPK1 (B) and DAPK3 (D) were measured in the presence of 1  $\mu$ M **6** (●) or vehicle (○).

the other 48 serine/threonine- or tyrosine-kinases tested to date. Furthermore, compounds with the structure of 4-(pyridin-3-ylmethylene)oxazol-5(4*H*)-one indicated similar selectivity in the same assay.

## Conclusions

Structure-based virtual screening was carried out to identify novel DAPK inhibitors using CONSENSUS-DOCK. Nearly 400 000 compounds were docked and ranked by consensus score. Initially, 100 compounds were selected for the DAPK inhibition assay and we identified four novel inhibitors. In a further similarity search based on the structure of **3**, we identified the most potent and selective DAPK inhibitor

**Table 3.** Kinase Selectivity of Compound **6** As Determined in Broad Protein Kinase Panel Screening

no inhibition at 10 $\mu$ M			
ABL	Erk1	MARK1	PKC $\zeta$
AKT1	FLT3	MAPKAPK2	PKD2
AKT2	FYN	MET	PKG $\alpha$
AMPK	GSK3 $\beta$	MSK1	PRAK
AurA	HGK	MST2	ROCK2
BTK	IGF1R	p38 $\alpha$	RSK1
CAMK2	INSR	PAK2	SRC
CAMK4	IRAK4	PIM2	SYK
CDK2	LCK	PKA	c-TAK1
CHK1	LYN	PKC $\beta$ 2	c-Raf
CHK2			
IC <sub>50</sub> > 10 $\mu$ M		1 $\mu$ M < IC <sub>50</sub> < 10 $\mu$ M	
CK1 $\delta$	FGFR1	p70S6K	DAPK1
DYRK1 $\alpha$	KDR		DAPK3
Erk2	SGK1		

known to date (**6**; IC<sub>50</sub> = 69 nM for DAPK1). These successful results indicate that structure-based virtual screening increases the efficiency of identifying active compounds among large numbers of compounds, particularly compared to high-throughput screening. The novel, potent, and selective DAPK inhibitors reported here will contribute to the development of new therapeutic approaches for the treatment of ischemic diseases in brain, heart, kidneys, and other organs.

## Experimental Section

The database of commercially available compounds was produced by Namiki Shoji Co., Ltd. (<http://www.namiki-s.co.jp/>) and included compounds produced by several suppliers. Tested compounds in this paper were purchased from several suppliers (e.g., Enamine, Pharmeks, Labotest). Their characterizations were confirmed using <sup>1</sup>H NMR and ESI-MS, and their purity was greater than 95% as determined by HPLC.

**Kinase Assay.** Kinase assay was performed using the Z'-LYTE kinase assay kit Ser/Thr 13 peptide (Invitrogen, Carlsbad, CA). The standard reaction for compound screening contained 1 mM peptide substrate, 10 mM ATP, 50 mM HEPES (pH 7.4), 10 mM MgCl<sub>2</sub>, 0.01% Brij-35, and 0.5% DMSO. Human recombinant DAPK1 (Invitrogen) was used at a final concentration of 2.6  $\mu$ g/mL, and recombinant DAPK3 (Invitrogen) was used at a final concentration 1.5 mg/mL. To test the enzyme selectivity of the inhibitors, ProfilerPro kits (Caliper Life Sciences, Inc., Hopkinton, MA) were used as described in the protocol.

**Note Added after ASAP Publication.** This paper was published on October 30, 2009 with an error in Table 1 and the caption of Figure 5. The revised version was published on November 4, 2009.

**Supporting Information Available:** Comparison of enrichment curves for CONSENSUS-DOCK versus DOCK4 only. This material is available free of charge via the Internet at <http://pubs.acs.org>.

## References

- Shohat, G.; Shani, G.; Eisenstein, M.; Kimchi, A. The DAP-kinase family of proteins: study of a novel group of calcium-regulated death-promoting kinases. *Biochim. Biophys. Acta* **2002**, *1600*, 45–50.
- Gozuacik, D.; Kimchi, A. DAPK protein family and cancer. *Autophagy* **2006**, *2* (2), 74–79.
- Velentza, A. V.; Schumacher, A. M.; Weiss, C.; Egli, M.; Watterson, D. M. A protein kinase associated with apoptosis and tumor suppression. *J. Biol. Chem.* **2001**, *276*, 38956–38965.

- (4) Shamloo, M.; Soriano, L.; Wieloch, T.; Nikolich, K.; Urfer, R.; Oksenberg, D. Death-associated protein kinase is activated by dephosphorylation in response to cerebral ischemia. *J. Biol. Chem.* **2005**, *280*, 42280–42299.
- (5) Velentza, A. V.; Wainwright, M. S.; Zasadzki, M.; Mirzoeva, S.; Schumacher, A. M.; Haiech, J.; Focia, P. J.; Egli, M.; Watterson, D. M. An aminopyridazine-based inhibitor of a pro-apoptotic protein kinase attenuates hypoxia-ischemia induced acute brain injury. *Bioorg. Med. Chem. Lett.* **2003**, *13*, 3465–3470.
- (6) Ewing, T. J.; Kuntz, I. D. Critical evaluation of search algorithms for automated molecular docking and database screening. *J. Comput. Chem.* **1997**, *18*, 1175–1189.
- (7) Rarey, M.; Kramer, B.; Lengauer, T.; Klebe, G. A fast flexible docking method using an incremental construction algorithm. *J. Mol. Biol.* **1996**, *261*, 470–489.
- (8) Muegge, I.; Martin, Y. C. A general and fast scoring function for protein–ligand interactions: a simplified potential approach. *J. Med. Chem.* **1999**, *42*, 791–804.
- (9) Charifson, P. S.; Corkery, J. J.; Murcko, M. A.; Walters, P. Consensus scoring: a method for obtaining improved hit rates from docking databases of three-dimensional structures into proteins. *J. Med. Chem.* **1999**, *42*, 5100–5109.
- (10) We used a database of commercially available compounds from several suppliers produced by Namiki Shoji Co., Ltd. (<http://www.namiki-s.co.jp/>). This database is supplied in a MOE molecular database file by Ryoka Systems Inc. (<http://www.rsi.co.jp/>).
- (11) Tereshko, V.; Teplova, M.; Brunzelle, J.; Watterson, M.; Egli, M. Crystal structures of the catalytic domain of human protein kinase associated with apoptosis and tumor suppression. *Nat. Struct. Biol.* **2001**, *8*, 899–907.
- (12) *Molecular Operating Environment (MOE 2006.0801)*; Chemical Computing Group Inc., 1255 University Street, Suite 1600, Montreal, Quebec H3B 3X3, Canada.
- (13) Fabian, M. A.; Biggs, W. H., III; Treiber, D. K.; Atteridge, C. E.; Azimioara, M. D.; Benedetti, M. G.; Carter, T. A.; Ciceri, P.; Edeen, P. T.; Floyd, M.; Ford, J. M.; Galvin, M.; Gerlach, J. L.; Grotzfeld, R. M.; Herrgard, S.; Insko, D. E.; Insko, M. A.; Lai, A. G.; Lelias, J.-M.; Mehta, S. A.; Milanov, Z. V.; Velasco, A. M.; Wodicka, L. M.; Patel, H. K.; Zarrinkar, P. P.; Lockhart, D. J. A small molecule–kinase interaction map for clinical kinase inhibitors. *Nat. Biotechnol.* **2005**, *23*, 329–336.
- (14) Horio, K.; Muta, H.; Goto, J.; Hirayama, N. A simple method to improve the odds in finding “lead-like” compounds from chemical libraries. *Chem. Pharm. Bull.* **2007**, *55*, 980–984.
- (15) Sadowski, J.; Gasteiger, J.; Klebe, G. Comparison of automatic three-dimensional model builders using 639 X-ray structures. *J. Chem. Inf. Comput. Sci.* **1994**, *34*, 1000–1008. CORINA is available from Molecular Networks GmbH, Erlangen, Germany (<http://www.molecular-networks.com/>).
- (16) Hensen, C.; Hermann, J. C.; Nam, K.; Ma, S.; Gao, J.; Holtje, H.-D. A combined QM/MM approach to protein–ligand interactions: polarization effects of the HIV-1 protease on selected high affinity inhibitors. *J. Med. Chem.* **2004**, *47*, 6673–6680.